

## Predictions of High Energy Experimental Results

Eliahu Comay

Charactell Ltd., PO Box 39019, Tel-Aviv, 61390, Israel. E-mail: elicomay@post.tau.ac.il

Eight predictions of high energy experimental results are presented. The predictions contain the  $\Sigma^+$  charge radius and results of two kinds of experiments using energetic pionic beams. In addition, predictions of the failure to find the following objects are presented: glueballs, pentaquarks, Strange Quark Matter, magnetic monopoles searched by their direct interaction with charges and the Higgs boson. The first seven predictions rely on the Regular Charge-Monopole Theory and the last one relies on mathematical inconsistencies of the Higgs Lagrangian density.

### 1 Introduction

A person who studies a well established physical theory becomes acquainted with its mathematical structure and with results of key experiments that are consistent with it. Here one generally does not pay much attention to the historical order of the development of theory and experiment. The situation is different in the case of a theory which has not yet passed the test of time. In the case of such a theory, one generally compares its conclusions with already known experimental results. However, in this situation, experiments that have not yet been performed play a specific role and one is generally inclined to be convinced of the theory's merits, if it predicts successfully experimental results that are obtained later.

This work describes eight predictions of high energy experimental results. All but one of the predictions rely on the Regular Charge-Monopole Theory (RCMT) [1, 2] and on its application to hadronic structure and processes [3]. From this point of view, the prediction of the failure to find a genuine Higgs boson makes an exception, because it relies on the inherently problematic structure of the Higgs Lagrangian density [4]. Some of the predictions refer to experiments that have not yet been carried out, whereas others refer to experiments that are performed for decades and failed to detect special objects. The second set contains the search for a monopole by means of its direct interaction with charge, glueballs, pentaquarks, nuggets of Strange Quark Matter (SQM) and the Higgs boson. In spite of a long list of experimental attempts that have ended in vain, searches for these objects still continue. The predictions made herein state that genuine particles of these kinds will not be found.

The second section presents a detailed phenomenological calculation that yields a prediction of the charge radius of the  $\Sigma^+$  baryon. This outcome is higher than that of a QCD based prediction that has been published recently [5]. All other predictions are derived briefly or have already been published elsewhere. The third section contains a list of short descriptions of each of these predictions. Concluding remarks are included in the last section.

### 2 The $\Sigma^+$ charge radius

The prediction of the  $\Sigma^+$  charge radius relies on phenomeno-

Particle	Mass (MeV)	$\langle \rho r^2 \rangle$	$\langle r \rangle$	Error
$p$	938.3	0.766	0.875	
$n$	939.6	-0.116		
$\Sigma^-$	1197.4	-0.61	0.78	0.15
$\pi^+$	139.6	0.452	0.672	
$k^+$	493.7	0.314	0.56	

Table 1: Known mean square charge radius ( $\langle \rho r^2 \rangle$ ) and charge radius ( $\langle r \rangle$ ) of hadrons.

logical estimates of expectation value of spatial variables of baryonic quarks. Here the RCMT indicates a similarity between electrons in an atom and quarks in a baryons [3]. Appropriate phenomenological assumptions are explained and it is shown how their application yields the required prediction of the  $\Sigma^+$  charge radius. The procedure used herein relies on the currently known data of the proton, the neutron and the  $\Sigma^-$  baryons [6]. The  $\pi$  and the  $k$  meson data are used as a justification for the calculations.

Table 1 contains the presently known data of the mean square charge radius ( $\langle \rho r^2 \rangle$ ) and of the corresponding charge radius of several hadrons, written in units of  $fm$ .

Remarks: *The experimental error refers to  $\langle \rho r^2 \rangle$ . Here the error of the  $\Sigma^-$  data is much larger than that of the other baryons. Therefore, only the  $\Sigma^-$  error is mentioned. The  $\pi^-$  and  $k^-$  are antiparticles of their respective positively charged counterparts and have the same spatial data.*

The three valence quarks of baryons make an important contribution to the quantities described in Table 1. Beside these quarks, it is well known that pairs of  $\bar{q}q$  are found in baryons. The graphs of Fig. 1 describe the distribution of quarks and antiquarks in the proton. Two physically important properties of the proton (and of all other baryons) are inferred from the data of Fig. 1.

- A. Antiquarks (namely, additional  $\bar{q}q$  pairs) are explicitly seen in baryons and their probability is not negligible.
- B. The  $x$ -width of antiquarks is much smaller than that of quarks. This property also proves that the Fermi motion of antiquarks is much smaller than that of quarks. Using the Heisenberg uncertainty principle, one finds that,

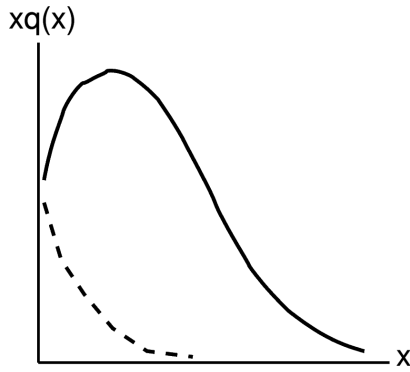


Fig. 1: The quantity  $xq(x)$  describes qualitatively as a function of  $x$  ( $q(x)$  denotes quark/antiquark distribution, respectively). The solid line represents quarks and the broken line represents antiquarks. (The original accurate figure can be found on [7, see p. 281]).

in a baryon, the volume of antiquarks is much larger than that of quarks.

These conclusions are called below Property A and Property B, respectively.

Property B is consistent with the RCMT hadronic model [3]. Indeed, in this model baryons have a core. The model assigns three positive monopole units to the baryonic core and one negative monopole unit to every quark. Now, by analogy with the electronic structure of atoms, one infers that, at the inner baryonic region, the potential of the baryonic core is not completely screened by quarks. For this reason, antiquarks, whose monopole unit has the same sign as that of the baryonic core, are pushed out to the baryonic external region and are enclosed inside a larger volume. (Property B is not discussed in QCD textbooks.)

An evaluation of experimental data of the proton indicates that the  $u, d$  quark flavors make the dominant contribution to the  $\bar{q}q$  pairs and that, in the proton, the ratio between the probability of these kinds of quarks is [8]

$$\frac{\langle \bar{d} \rangle}{\langle \bar{u} \rangle} \approx 3/2. \quad (1)$$

This ratio is used later in this work. Obviously, isospin symmetry shows that this ratio is reversed for the neutron. The excess of the additional  $\bar{d}d$  quark pairs in the proton is consistent with the Pauli exclusion principle, which RCMT ascribes to the spin-1/2 quarks. Indeed, a proton contains  $uud$  valence quarks. Hence, it is energetically easier to add a  $\bar{d}d$  pair than a  $\bar{u}u$  pair.

The following assumption relies on Property A of Fig. 1.

- I. It is assumed that, on the average, a baryon contains one additional  $\bar{q}q$  pair. Thus, in the discussion carried out below, baryons contain four quarks and one antiquark. In particular, a proton contains an additional 0.6  $\bar{d}d$  fraction of a pair and 0.4  $\bar{u}u$  fraction of a pair. Isospin symmetry indicates that for a neutron, the corresponding quantities are reversed.

The calculation of the baryonic *charge radius* is not very sensitive to the accuracy of Assumption I. Indeed, each member of a  $\bar{q}q$  has an opposite electric charge and their contributions partially cancel each other. Moreover, the  $ud$  quarks carry charge of opposite sign. This property further reduces the effect of the additional pairs. The discussion of the neutron data, which is carried out later, illustrates these issues.

The baryonic mean square charge radius is obtained below as a sum of the contribution of the baryon's individual quarks. Thus, the following notation is used for a quark  $q$  and a baryon  $b$

$$R^2(q_i, b) \equiv \int r^2 \psi_i^\dagger \psi_i d^3x, \quad (2)$$

where  $\psi_i^\dagger \psi_i$  represents the single particle density of a  $q_i$  quark. (Below,  $\psi$  is not used explicitly, and the value of  $R^2(q, b)$  is derived phenomenologically from the data of Table 1.) Thus,  $R^2(u, p)$  denotes the value of (2) for one of the proton's  $u$  quarks. Analogous expressions are used for other quark flavors and for other baryons. It follows that the contribution of each quark to the baryonic *mean square charge radius* is obtained as a product  $QR^2(q, b)$ , where  $Q$  denotes the charge of the respective quark. Relying on isospin symmetry, one defines Assumption II:

$$R^2(u, p) = R^2(d, p) = R^2(u, n) = R^2(d, n) \equiv R^2, \quad (3)$$

where the last symbol is used for simplifying the notation.

As explained above, both the data depicted in Fig. 1 and the RCMT model of hadrons [3], indicate that the volume of baryonic antiquarks is larger than that of the corresponding quarks (herein called Property B). Therefore, by analogy of (3), the following definition is used for the proton/neutron antiquarks

$$R^2(\bar{u}, p) = R^2(\bar{d}, p) = R^2(\bar{u}, n) = R^2(\bar{d}, n) = \lambda R^2, \quad (4)$$

where  $\lambda > 1$  is a numerical parameter.

The foregoing arguments and the data of Table 1 enable one to equate the experimental value of the proton's mean square charge radius with the quantities defined above

$$\begin{aligned} 0.766 &= 2 \frac{2}{3} R^2 - \frac{1}{3} R^2 - 0.4(\lambda - 1) \frac{2}{3} R^2 + 0.6(\lambda - 1) \frac{1}{3} R^2 = \\ &= R^2 - 0.2(\lambda - 1) \frac{1}{3} R^2. \end{aligned} \quad (5)$$

The terms on the right hand side of the first line of (5) are defined as follows. The first term represents the contribution of the two  $uu$  valence quarks; the second term is for the single  $d$  quark; the third term is for the  $\bar{u}u$  pair; the last term is for the  $\bar{d}d$  pair.

An analogous treatment is applied to the neutron and the result is

$$\begin{aligned} -0.116 &= \frac{2}{3} R^2 - 2 \frac{1}{3} R^2 - 0.6(\lambda - 1) \frac{2}{3} R^2 + 0.4(\lambda - 1) \frac{1}{3} R^2 = \\ &= -0.8(\lambda - 1) \frac{1}{3} R^2. \end{aligned} \quad (6)$$

Here one sees once again the merits of the RCMT model of hadrons [3]. Thus, the fact that the proton's antiquarks volume is larger than that of its quarks means that  $\lambda > 1$ , as seen in (4). Obviously, the final result of (6) proves that this relation is mandatory for explaining the *sign* of the experimental value of the neutron's mean square charge radius. It is also evident that the contribution of the quark-antiquark pair to  $R^2$  is small.

The neutron relation (6) enables the removal of the  $\lambda$  parameter from (5). Thus, one finds that

$$R^2 = 0.766 + 0.116/4 = 0.795. \quad (7)$$

This value of  $R^2$  will be used in the derivation of the prediction for the charge radius of the  $\Sigma^+$  baryon.

Let us turn to the  $\Sigma^-$  baryon whose valence quarks are  $dds$ . The  $u, d$  quarks of the previous discussion are regarded as particles having (practically) the same mass and a different electric charge. This is the underlying basis of isospin symmetry. It is also agreed that the  $s$  quark is heavier. Indeed, the following data support this statement. Thus, the experimental mass difference (in MeV) of the  $k, \pi$  mesons is [6]

$$M(k^+) - M(\pi^+) = 493.7 - 139.6 = 354.1 \quad (8)$$

and the difference between the isospin average of the  $\Sigma^\pm$  and the nucleons is

$$\begin{aligned} \frac{1}{2} (M(\Sigma^+) + M(\Sigma^-) - M(p) - M(n)) &= \\ = \frac{1}{2} (1197.4 + 1189.4 - 938.3 - 939.6) &= 254.5. \end{aligned} \quad (9)$$

In each of the previous relations, the mass difference between two hadrons, where an  $s$  quark replaces a  $u$  (or  $d$ ) quark is positive. This outcome indicates that the  $s$  quark is indeed heavier than the  $u$  quark.

The RCMT model of baryons and mesons [3] is analogous to the atomic structure of electrons and to the positronium, respectively. The results of (8) and (9) show that replacing a  $u$  (or  $d$ ) quark by an  $s$  quark in a nucleon yields more binding energy than doing it in a pion. This outcome is consistent with the RCMT model. Indeed, in a meson, an  $s$  quark is attracted just by the field of one antiquark that carries *one* monopole unit. On the other hand, in a nucleon, the  $s$  quark is attracted by the baryonic core that carries *three* monopole units. Like in the atomic case, the field of the core is not completely screened by the other quarks. (A QCD explanation of this phenomenon is certainly less obvious.)

Let us turn to the problem of the  $s$  quark single particle radial distribution. Thus, if a  $u$  (or  $d$ ) quark is replaced by the heavier  $s$  quark, then the  $s$  quark mean radius will be smaller than that of the  $u$  quark. This conclusion is supported both by the mass dependence of the radial function of a Dirac solution of the Hydrogen atom (see [9, see p. 55] and by a comparison

of the experimental  $k$  and  $\pi$  radii of Table 1. For this reason, it is defined here that

$$R^2(s, \Sigma^-) = \eta R^2, \quad (10)$$

where  $0 < \eta < 1$  is a yet undefined parameter.

By analogy with the case of atomic electrons, one should expect that the negative monopole of the  $s$  quark, which is closer to the core, partially *screens* the potential of the positive monopole at the baryonic core. Therefore, one may expect a somewhat larger size for the  $d$  quarks of the  $\Sigma^-$  baryon

$$R^2(d, \Sigma^-) = \xi R^2, \quad (11)$$

where  $\xi > 1$  is another undefined parameter.

Like the neutron, whose valence quarks are  $udd$ , the  $\Sigma^-$  valence quarks  $dds$  contains a pair of  $d$  quarks. Hence, it is assumed here that the contribution of a quark-antiquark pair to the  $\Sigma^-$  mean square charge radius is the same as that of the neutron (6). (As shown above, the contribution of this effect is relatively small, and the final result is not sensitive to a small change of this quantity.) Taking the experimental value of the  $\Sigma^-$  from Table 1, one uses (6), (7), (10), and (11) and writes the following relation for the two undetermined parameters  $\xi, \eta$

$$-0.61 \pm \delta = -2 \frac{1}{3} 0.795 \xi - \frac{1}{3} 0.795 \eta - 0.116, \quad (12)$$

where  $\delta$  is related to the error assigned to the measurement of the mean square charge radius of the  $\Sigma^-$  baryon (see Table 1).

Taking into account the constraint on  $\xi, \eta$ , one finds that relation (12) does not hold for  $\delta = 0$ . Table 2 describes some pairs of values of the parameters  $\xi, \eta$  and their relation to  $\delta$ . It is shown below how each pair of the  $\xi, \eta$  parameters of Table 2 yields a prediction of the  $\Sigma^+$  mean square charge radius.

The  $\Sigma^+$  baryon contains the  $uus$  valence quarks and it is the isospin counterpart of the  $\Sigma^-$  baryon. Hence, the spatial properties of its  $u$  quarks are the same as those of the  $d$  quarks of the  $\Sigma^-$  baryon. Also the  $s$  quark of these baryons is assumed to have the same spatial properties. The small effect of the quark-antiquark pairs is equated to that of the proton, because both have a pair of  $uu$  valence quarks. Thus, the phenomenological formula for the mean square charge radius of the  $\Sigma^+$  baryon is

$$R^2(\Sigma^+) = 2 \frac{2}{3} 0.795 \xi - \frac{1}{3} 0.795 \eta - 0.029, \quad (13)$$

where  $R^2(b)$  denotes the mean square charge radius of the baryon  $b$ . Substituting the values of each pair of the parameters  $\xi, \eta$  into (13), one obtains a predictions for  $R^2(\Sigma^+)$ . It is clear from the details of the discussion presented above that a prediction of  $R^2(\Sigma^+)$  must carry the estimated experimental error of the mean square charge radius of the  $\Sigma^-$  baryon *and*

$\delta$	$\xi$	$\eta$
-15	1.0	0.43
-15	1.05	0.33
-15	1.1	0.23
-10	1.12	0.0
-5	1.03	0.0

Table 2: Several values of  $\xi$  and  $\eta$  of (12).

the uncertainties of the assumptions used herein. Thus, the final prediction is given (in  $fm^2$ ):

$$0.85 \leq R^2(\Sigma^+) \leq 1.17. \quad (14)$$

The prediction for the charge radius (in  $fm$ ) is

$$0.91 \leq R(\Sigma^+) \leq 1.12. \quad (15)$$

The range of these predictions is higher than that of a QCD dependent prediction which has been published recently [5].

### 3 The other seven high energy predictions

This section presents seven predictions of high energy experimental results.

- High Energy pion beams exist. Thus, in principle, the experiment described here can be performed in the near future. The RCMT basis for a prediction of the elastic  $\pi - \pi$  cross section is explained. Unlike protons (see [10] and references therein), pions are characterized by a pair of quark-antiquark and *they do not have inner quark shells*. Moreover, in a deep inelastic  $e - p$  experiment, the electron collides with one quark at a time. This property should also hold for the quark-quark interaction in a  $\pi - \pi$  collision. Therefore, relying on RCMT, where quarks carry one monopole unit, the  $\pi - \pi$  elastic cross section is analogous to the elastic cross section of colliding charges. It is well known that this cross section decreases with the increase of the collision energy (see chapter 6 of [7]).

Prediction: Unlike the proton case, where the elastic cross section increases for collision energy which is greater than that of point C of Fig. 2, a decrease of the elastic cross section is predicted for a  $\pi - \pi$  scattering. Hence, its graph will not increase for energies which are not too close to a resonance. In particular, no similar effect like the rise of the  $p - p$  cross section on the right hand side of point C will be found in a  $\pi - \pi$  collision. By the same token, for a very high energy  $\pi - \pi$  scattering, the ratio of the elastic cross section to the total cross section will be much smaller than that of the  $p - p$  cross section of Fig. 2, which is about 1/6.

- The problem of the portion of the pion's momentum carried by quarks. The deep inelastic  $e - p$  scattering data are used for calculating the relative portion of

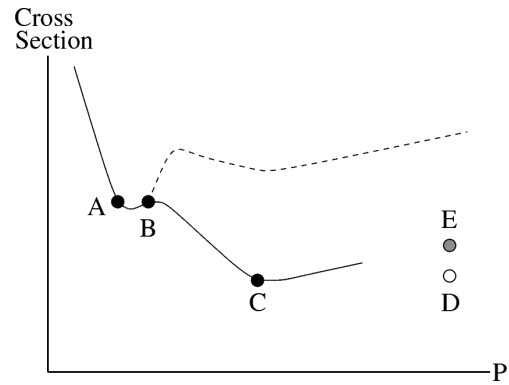


Fig. 2: A qualitative description of the pre-LHC proton-proton cross section versus the laboratory momentum P. Axes are drawn in a logarithmic scale. The solid line denotes the elastic cross section and the broken line denotes the total cross section. (The accurate figure can be found in [6].)

the proton's momentum carried by quarks, as seen in a frame where the proton's momentum is very very large. It turns out that for a proton, the overall quarks' portion is about one half of the total momentum. The RCMT proves that baryons have a core and that this is the reason for the effect. Mesons are characterized as a bound  $\bar{q}q$  pair and they *do not have a core*. This is the basis for the following prediction:

Unlike the proton case, it is predicted that an analogous experiment of deep inelastic  $e - \pi$  scattering will prove that in this case the pion's quarks carry all (or nearly all) the pion's momentum.

- Several decades ago, claims concerning the existence of glueballs have been published by QCD supporters (see [11], p. 100). RCMT describes the strong interactions as interactions between monopoles that satisfy the RCMT equations of motion. Here, no gluon exist. A fortiori, a genuine glueball does not exist. On April 14, 2010, Wikipedia says that glueballs "have (as of 2009) so far not been observed and identified with certainty."
- Several decades ago, claims concerning the existence of pentaquarks have been published by QCD supporters [12, 13]. Pentaquarks are supposed to be strongly bound states of a baryon and a meson. RCMT clearly contradicts the existence of these kinds of objects. Indeed, like nucleons, all hadrons are neutral with respect to monopoles. Hence, like the nuclear force, a hadron-hadron interaction has residual features. In a deuteron the proton-neutron binding energy is about 2.2 MeV. Let us compare this value to what is expected for a baryon-meson binding energy. For each flavor, the lightest meson, which is the best candidate for assembling a pentaquark, is a spin-0 particle, which resembles a noble gas. Hence, the binding energy of a nucleon with this kind of meson should be even smaller

than the 2.2 MeV binding energy of the deuteron. For this reason, strongly bound pentaquarks should not exist. Experimental results are consistent with this theoretical conclusion [14].

- Several decades ago, claims concerning the existence of SQM have been published by QCD supporters [15]. RCMT clearly contradicts the existence of this kind of matter. Indeed, an SQM is a nugget of  $\Lambda$  baryons. Now the mass of a  $\Lambda$  baryon is greater than the nucleon mass by more than 170 MeV. On the other hand, the  $\Lambda$  binding energy in an SQM should be similar to the nucleon binding energy in a nucleus, which is about 8 MeV per nucleon. This very large difference between energy values proves that the SQM is unstable and will disintegrate like a free  $\Lambda$ . Experimental results are consistent with this theoretical conclusion [16].
- RCMT proves that there is no *direct* charge-monopole interaction. Radiation fields (namely, real photons) interact with charges *and* with monopoles. As of today, experimental attempts to detect monopoles rely on a direct interaction of the monopole fields with charges of the measuring device. As stated above, such an interaction does not exist. Hence, no genuine monopole will be detected. This prediction has been made about 25 years ago [17]. In spite of a very long search, all attempts to detect monopoles have ended in vain [6, see p. 1209]. Monopole search continues [18].
- A genuine Higgs boson will not be found. For a theoretical discussion, see the first four sections of [4]. This conclusion relies on inherent inconsistencies of the Higgs Lagrangian density.

#### 4 Concluding remarks

A physical theory is tested by its consistency with experimental results that belong to the theory's domain of validity. A second kind of test is the demand that the examined theory has a solid mathematical structure. However, one does not really think that a theory having an erroneous mathematical structure can fit all experimental data. Therefore, one may argue that a test of the theory's mathematical structure plays an auxiliary role. On the other hand, an analysis of the mathematical structure can provide convincing arguments for disqualifying incorrect theories. The present work concentrates on the examination of the fit of high energy theories to the data.

In undertaking this task, one realizes that the historical order of formulating the theory's predictions and carrying out the required experiments bears no fundamental meaning. Thus, at this point, one may state that making a prediction that is later found to be successful is *at least* as good as deriving a theoretical result that fits a known measurement. This is certainly an incomplete description of the problem. Indeed,

many predictions depend on numerical value of adjustable parameters that yield the required quantity. Therefore, in the case of a theory that is not fully established, a successful prediction that is *later* confirmed by measurement provides a significantly better support for it. This aspect is one of the motivations for writing the present work which contains eight different predictions. Let us wait and see what will come out of the experimental work.

Submitted on April 19, 2010 / Accepted on April 23, 2010

#### References

1. Comay E. Axiomatic deduction of equations of motion in Classical Electrodynamics. *Nuovo Cimento B*, 1984, v. 80, 159–168.
2. Comay E. Charges, Monopoles and duality relations. *Nuovo Cimento B*, 1995, v. 110, 1347–1356.
3. Comay E. A regular theory of magnetic monopoles and its implications. In: *Has the Last Word Been Said on Classical Electrodynamics?* Editors: Chubykalo A., Onoochin V., Espinoza A.R. and Smirnov-Rueda R. Rinton Press, Paramus (NJ), 2004.
4. Comay E. Physical consequences of mathematical principles. *Prog. in Phys.*, 2009, v. 4, 91–98.
5. Wang P., Leinweber D.B., Thomas A.W. and Young R.D. Chiral extrapolation of octet-baryon charge radii. *Phys. Rev. D*, 2009, v. 79, 094001-1–094001-12.
6. Amsler C. et al. Review of particle physics. *Phys. Lett. B*, 2008, v. 667, 1–1340.
7. Perkins D.H. Introduction to high energy physics. Addison-Wesley, Menlo Park (CA), 1987.
8. Alberg M. Parton distributions in hadrons. *Prog. Part. Nucl. Phys.*, 2008, v. 61, 140–146.
9. Bjorken J.D. and Drell S.D. Relativistic quantum mechanics. McGraw-Hill, New York, 1964.
10. Comay E. On the significance of the upcoming large hadron collider proton-proton cross section data. *Prog. in Phys.*, 2010 v. 2, 56–59.
11. Frauenfelder H. and Henley E.M. Subatomic physics. Prentice Hall, Englewood Cliffs, 1991.
12. Gignoux C., Silvestre-Brac B. and Richard J.M. Possibility of stable multi-quark baryons. *Phys. Lett.*, 1987, v. 193, 323–326.
13. Lipkin H.J. New possibilities for exotic hadrons — anticharmed strange baryons. *Phys. Lett.*, 1987, v. 195, 484–488.
14. Whole C.G. (in the 2009 report of PDG). See: <http://pdg.lbl.gov/2009/reviews/rpp2009-rev-pentaquarks.pdf>
15. Witten E. Cosmic separation of phases. *Phys. Rev. D*, 1984, v. 30, 272–285.
16. Han K. et al. Search for stable strange quark matter in Lunar soil. *Phys. Rev. Lett.*, 2009, v.103, 092302-1–092302-4.
17. Comay E. Will magnetic monopoles be detected in our instruments? *Let. Nuovo Cimento*, 1985, v. 43, 150–152.
18. A monopole search is planned to be carried out at the LHC. See: <http://cdsweb.cern.ch/record/1243082>